ChemistrySelect

Research Article
doi.org/10.1002/slct.202400409

Chemistry Europe
European Chemical Societies Publishing

www.chemistryselect.org

# A Simplistic Label-Free Electrochemical Immunosensing Approach for Rapid and Sensitive Detection of Anti-SARS-COV-2 Nucleocapsid Antibodies

Branham J. Kock,[a] Jarid Du Plooy,[a] Rochida A. Cloete,[a] Nazeem Jahed,[a] Thuan Nguyen Pham-Truong,[b] Christopher Arendse,[c] and Keagan Pokpas*[a]

Rapid and precise detection of SARS-CoV-2 antibodies is paramount for effective outbreak monitoring and vaccine efficacy assessment. While existing approaches for antibody detection often rely on complex electrochemical immunosensing with nanomaterial functionalization targeting S-protein antibodies, their limitations in sensitivity and complexity have hindered widespread application. Here, we present a simplistic immunosensing platform designed for the rapid, and precise detection of SARS-CoV-2 specific IgG and Nucleocapsid antibodies. Notably, this study marks only the second exploration of SARS-CoV-2 N-protein antibody detection. The platform utilizes traditional self-assembled monolayers to establish selective bioaffinity between SARS-CoV-2 specific Nucleocapsid antibodies and a gold electrode functionalized with the N-protein antigen. Interestingly, despite the absence of nanomaterial functionalization, the developed platform achieves sensitivity comparable to existing sensors across a wide detection range (0.025 to 1 ng/mL) with an impressive limit of detection (0.019 ng/mL). The simplicity of the approach, relying solely on immunocomplex reactions, underscores that effective binding efficiency may be achieved in the absence of complex functionalization and determines its affordability, specificity, and high sensitivity. By eliminating the need for additional functionalization steps, the platform offers a streamlined solution for SARS-CoV-2 antibody detection and demonstrates the possibility of N-protein antibody detection as a promising avenue for widespread application in SARS-CoV-2 outbreak monitoring and vaccine efficacy assessment particularly in underdeveloped regions.

## Introduction

The most recent global threat to our well-being is the rapid spread of Coronavirus Disease 2019 (Covid-19), a respiratory illness caused by a large RNA virus known as the coronavirus. This enveloped virus has a positive single-stranded RNA genome, making it capable of infecting humans. Individuals afflicted with Covid-19 typically exhibit symptoms such as fever, cough, nasal congestion, and various other indicators of upper respiratory tract infections. In more advanced stages of the infection, when the patient's condition deteriorates, pneumonia may develop characterized by its distinct symptoms. To mitigate the impact of Covid-19 symptoms and potentially confer immunity, various vaccines have been developed.[1]

Current diagnostic methods for SARS-CoV-2 include Antigen tests, Nucleic Acid Amplification Tests (NAATs), and other viral tests. The predominant clinical diagnostic tool for the coronavirus is the Quantitative Reverse Transcription-Polymerase Chain Reaction (qRT-PCR), which targets the E and RdRP genes of the virus.[2] While qRT-PCR has proven its utility, it is not without limitations. For instance, in asymptomatic patients, viral loads may be insufficient for accurate monitoring. Additionally, the presence of interfering substances may lead to false-positive results. Moreover, this method entails a relatively lengthy turnaround time, atypically ranging from 2–4 hours to obtain a result.[3]

Electrochemical detection has shown great promise to address the limitations of molecular spectroscopic approaches. A variety of electrochemical biosensors[4] have been developed for the detection of SARS-CoV-2, encompassing immunosensors,[5] aptasensors,[6] and enzymatic[7] sensors. These sensors utilize diverse platforms and substrates such as screen-printed electrodes (SPEs),[8] paper-based systems,[9,10] gold electrodes,[11] test strips,[12] and others, demonstrating rapid and accurate detection of SARS-CoV-2. Electrochemical sensing methods have gained prominence in detecting proteins, nucleic acids, bacteria, viruses, antibodies, and their fragments owing to their simplicity, low cost, rapidity, high sensitivity, and selectivity. In the context of SARS-CoV-2 detection, immunosen-

[a] B. J. Kock, J. Du Plooy, R. A. Cloete, N. Jahed, K. Pokpas
SensorLab, Chemistry Department
University of the Western Cape
Robert Sobukwe Road, Bellville, 7535, South Africa
Tel: +27 21 959 4038
E-mail: kpokpas@uwc.ac.za

[b] T. Nguyen Pham-Truong
CY LPPI - Laboratory of Physical Chemistry of Polymers and Interfaces
CY Cergy Paris Université
5 mail Gay Lussac, F-95000 Neuville sur Oise, France

[c] C. Arendse
Physics Department
University of the Western Cape
Robert Sobukwe Road, Bellville, South Africa, 7535

Supporting information for this article is available on the WWW under https://doi.org/10.1002/slct.202400409

sors operate by detecting a specific target analyte, such as an antigen (Ag), through the formation of a stable immunocomplex with an antibody acting as a capture agent (Ab). This interaction generates a quantifiable signal through a transducer, defining a biosensor as an immunosensor. In immunoassays, the system relies on the interaction between the antibody and the antigen, while in contrast, in immunosensors the development of the immunocomplex and diagnosis occur on the same platform. This is a nuanced distinction between immunosensors and immunoassays[13][14]. Antigen-antibody interactions are the focal point of recent research. The bulk of studies leverages these for the ultrasensitive detection of antigens. A less common approach is for the detection and monitoring of antibody production.[15] The structural composition of SARS-CoV-2 consists of 4 proteins, the spike protein, the membrane protein, the Envelope protein, and the Nucleocapsid Protein. These structural proteins found in SARS-CoV-2, differ most from their respective proteins in SARS-CoV and MERS-CoV viruses. Based on its ability to make a SARS-CoV-2 specific detection platform and its previously demonstrated high immunogenicity in similar devices, the nucleocapsid protein (N-Protein) has shown promise to be used as the biosensor's antigen. The N-protein to nucleocapsid antibody (N-antibody) interaction is more selective and sensitive for biosensor application in comparison to the commonly used spike protein. For the electrochemical biosensor referenced to be fabricated, a closer look into the Nucleocapsid protein (N) is discussed.[16]

The N-protein in question is one of the most abundant structural proteins in virus-infected cells and is highly conserved in the coronavirus genus.[17] The N-protein's primary function is to bundle the viral genome RNA into a long helical ribonucleocapsid (RNP) complex and engage in virion formation via interactions with the viral genome and membrane protein.[18] Furthermore, in host immunological reactions, the N protein is an immunodominant antigen that can be exploited as a diagnostic antigen and immunogen.[19]

Various researchers have explored antibody detection through electrochemical methods, with successful applications reported. Electrochemical impedance spectroscopy has been particularly effective in detecting SARS-CoV-2 antibodies using a nanowire-based biosensor, achieving a limit of detection (LOD) in the pg/mL range.[20] Najjar et al. proposed an innovative approach for antibody detection through RNA.[21] Their method involved an electrode functionalized with the Spike S1, nucleocapsid, and receptor-binding domain antigens of SARS-CoV-2. This setup facilitated the automatic extraction, concentration, and amplification of SARS-CoV-2 RNA from unprocessed saliva. It also integrated Cas12a-based enzymatic detection of SARS-CoV-2 RNA through isothermal nucleic acid amplification with a sandwich-based enzyme-linked immunosorbent assay. In contrast to other lateral flow-based assays (LFAs) that require multiple antibodies, a label-free paper-based electrochemical platform has been designed to target SARS-CoV-2 antibodies without the need for an additional antibody. This platform offers a distinct advantage in simplicity.[22] Additionally, a novel electrochemical sensor has demonstrated the rapid and label-free detection of SARS-CoV-2 antibodies using a commercially available impedance sensing platform. This method surpasses the standard enzyme-linked immunosorbent assay (ELISA) in terms of LOD and can effectively differentiate impedance spikes from negative control (1% milk solution) for all CR3022 samples.[23] These advancements showcase the versatility and efficacy of electrochemical approaches in the realm of SARS-CoV-2 antibody detection.

For the quick and precise measurement of SARS-CoV-2 serum antibodies, an electrochemical immunosensor that is portable and affordable was created. The immunosensor featured a quick test time, reported stable performance throughout a 24-week storage period at room temperature, and the ability to detect the quantities of immunoglobulin G (IgG) and immunoglobulin M (IgM) antibodies against the SARS-CoV-2 spike protein in human serum.[24] As a nanotool for the ultrasensitive selective quantitative analysis of SARS-CoV-2 antibodies, the spike protein was immobilized on the SPCE modified with nickel hydroxide nanoparticles ($Ni(OH)_2$ NPs). The addition of the NPs made the biodevice more stable and made the target detection more sensitive and selective.[25] Similarly, the immunosensor reported,[26] designed an Au immunosensor but detected for the S-Protein. The designed electrochemical immunosensor is suitable for verifying human COVID-19 immune response or infection following immunization. The analytical performance of immunosensors was greatly improved by adding synthetic peptides as selective recognition layers together with nanomaterials like gold nanoparticles (AuNPs). An electrochemical immunosensor built on a solid-binding peptide and tested for SARS-CoV-2 Anti-S antibodies was provided in the study. Two crucial components of the peptide employed as a recognition site were present: one based on the viral receptor binding domain (RBD), which can recognize antibodies of the spike protein (Anti-S), and another capable of interacting with gold nanoparticles.[27] Commercial electrical devices have also been modified to detect SARS-CoV-2.[28] The field of study continues to expand due to the few studies and Novelty behind the form of sensing.[29–31]

The majority of studies have primarily focused on detecting the spike protein.[32] Numerous sensor types have been designed with a specific emphasis on simplifying antigen detection. The overarching objective of these endeavors is to develop a smart sensor suitable for point-of-care (POC) applications in clinical analysis, providing patients with rapid and accessible clinical tests.[33] Adhering to these requirements, an ideal biosensor should possess several key attributes: good selectivity and stability,[34] rapid response,[35] a low limit of detection,[36] ease of use,[37] low cost,[38] and scalability. in contrast to previously reported SARS-CoV-2 biosensors, the developed immunosensor requires no additional modifications to enhance its detection properties. It has demonstrated its capability to detect in the low pg/mL range, effectively competing with the more complex biosensor designs.

Herein, a label-free electrochemical immunosensor utilizing commercial gold electrodes (AuE) as a straightforward and simplistic approach for antigen-antibody testing targeting SARS-CoV-2 nucleocapsid antibodies (N-antibody) is developed. While the monitoring of the antigen-antibody interaction for

Nucleocapsid Antibody detection has been relatively underexplored, it has proven to be a viable alternative for the detection of SARS-CoV-2. Here the design and optimization of a Au-based biosensor platform tailored for highly sensitive and selective detection of the SARS-CoV-2 nucleocapsid antigen was presented relying on conventional self-assembled monolayers. Two voltammetric methods, observing changes in current through differential pulse voltammetry (DPV) and electrochemical impedance spectroscopy (EIS), were employed in the detection process. The work represents an alternative to existing studies requiring platform functionalization with highly conductive materials and only the second of a handful of studies for monitoring of anti-SARS-CoV-2 nucleocapsid antibodies.

## Results and Discussion

### Functionalization and Characterization of Sars-Cov-2 Nucleocapsid Antibody Sensor

The Au sensor was produced by coating the gold working electrode with a self-assembled monolayer (SAM) of 25 MSA. The SAM creation severed to establish binding sites for the linker designed to interact specifically with the SARS-CoV-2 nucleocapsid protein. The approach used was similar to the work detailed in reference[39] and was meticulously characterized using electrochemical techniques as shown in Figure 1. To ensure the specificity of the sensing surface, excess reactive linkers were blocked by incubating the sensor with BSA. Subsequently, the sensor was utilized to measure the electrochemically active ferri/ferrocyanide reaction post-BSA blocking, providing a baseline or background signal. Following the blocking step, the sensor was subjected to analyte incubation, during which the designed linker facilitated the recognition and binding of the SARS-CoV-2 nucleocapsid protein to the sensor's surface-immobilized antibodies. The study underscores the importance of the sequential steps in creating a functional and selective sensing platform for the targeted detection of the SARS-CoV-2 nucleocapsid protein without the need for further modification with smart materials. The approach described herein holds promise for advancing the field of biosensing, particularly in the realm of infectious disease diagnostics.

Differential pulse voltammetry (DPV) and Electrochemical impedance spectroscopy (EIS) were performed to investigate the electrode behavior at different stages of surface modification, Figure 1A and 1B, respectively. DPV revealed distinct alterations in the ferri/ferrocyanide electron transfer kinetics throughout each modification step recorded between −0.4 and 0.8 V are shown in Figure 1A. A single, well-resolved peak is shown at 0.18 V for all surfaces studied attributed to the 1-electron transfer from $Fe(CN)_6^{3-}$ to $Fe(CN)_6^{4}$ . Carboxylic acid functionalities are introduced to the gold surface through MSA functionalization resulting in repulsion of the negatively charged Ferri/ferrocyanide ions. Subsequently, the carboxylic acid functionalized AuE may be activated following EDC/NHS chemistry. A slight increase in the $Fe(CN)_6^{3-/4-}$ peak current confirms this step. Notably, the introduction of N-protein and subsequent blocking with BSA induced a stepwise increase in electron-transport resistance shown by an approximate 25% and a further 60% decrease in peak current. The findings confirm the successful fabrication of the SARS-CoV-2 Nucleocapsid sensor. Further immobilization of 1 ng/mL test solutions of anti-SARS-CoV-2 specific N-protein antibodies was studied. A decrease in recorded peak current is observed demonstrating successful binding of biological antibodies at the sensor surface. Thus, these modifications acted as inert electron transfer-relating blocking layers without entirely hindering the diffusion of the ferri/ferrocyanide redox couple toward the electrode surface.

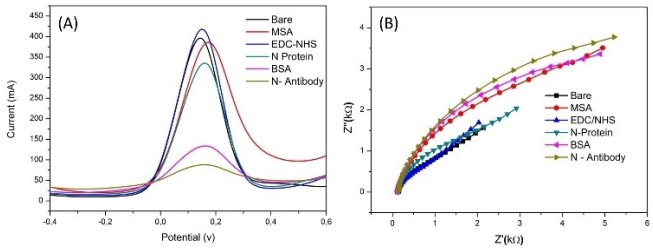


**Figure 1.** (A) Voltammograms of functionalized gold electrode detecting 1 ng/mL SARS-CoV-2 nucleocapsid antibody, and (B) EIS plot of functionalized gold electrode with 1 ng/mL SARS-CoV-2 nucleocapsid antibody 5 mM ($[Fe(CN)_6]^{3-/4-}$).

Subsequent characterization via electrochemical impedance spectroscopy delved deeper into the nuances of each electrode alteration stage. The Nyquist plots generated during the multiple functionalization steps are shown in Figure 1B and elucidate the evolving electron-transfer resistance. The EIS data was recorded in a frequency range between 1 and 10,000 Hz. An increase in calculated charge transfer resistance ($R_{ct}$) was found following, MSA, EDC/NHS, N-protein, and BSA functionalization. As seen in Figure 1B, one can observe a gradual increase in the diameter of the semicircle in the Nyquist plots when the relevant modifications were made. In this sense, it can indicate the inhibition effects of modified steps on the electron transfer between the redox probe and the electrode surface. This means that the interfacial properties can be altered even by little changes in the surface induced by specific binding to the surface of the AuE and ultimately with the N-Protein and N-Antibody. Immobilized antibodies on the electrode surface were found to distinctly obstruct electron transfer, indicative of the formation of an insulating barrier. The results are in agreement with those found in the voltammetric characterization. This detailed electrochemical analysis enhances our understanding of the intricacies involved in each surface modification step, confirming the efficient binding of bioreceptors and antigens for the detection of SARS-CoV-2 N-protein antibodies.

### Analytical Study for the Detection of the Nucleocapsid Antibody using the Electrochemical Immunosensor

The quantitative analysis of the Nucleocapsid antibody (N-antibody) detection was performed using DPV to detect a

change in the ferri/ferrocyanide signal. The N-protein functionalized working electrode was incubated for 30 min with varying concentrations of N-antibody between 0.01 and 10 ng/mL. DPV scans, spanning from −0.5 to 0.7 V, were performed before and after incubation of the target molecule. Analysis of the obtained signals involved point-by-point subtraction of the analyte peak from the background peak using PS Trace software. The subtraction yielded distinct peaks centred around 0.2 V, directly reflecting the contribution of the analyte to the overall electron diffusion. The calibration curve recorded by plotting the change in current vs concentration for the 0.01 and 10 ng/mL range is given in Figure 2. An increase in peak current with increasing concentration is exhibited up to approximately 2 ng/mL. Thereafter, saturation of the electrode surface with nucleocapsid antibody blocks redox reactions limiting change in current. A dynamic linear range of 0.025 and 1 ng/mL was found. The resulting voltammogram and corresponding calibration plots are provided in Figure 3A and 3B, respectively. A linear increase in change in peak current with increasing concentration is shown as peak currents are decreased. These peak heights served as a quantitative measure of the presence of the N-antibody, providing valuable insights into the effectiveness of the sensor in detecting varying concentrations of the target molecule. This DPV-based approach offers a robust and sensitive method for the quantitative analysis of N-antibody detection.

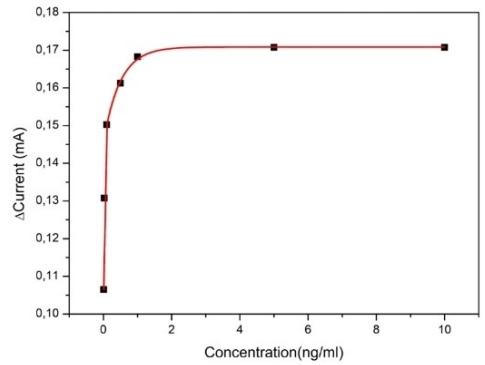


**Figure 2.** 7-point Calibration curve in varied concentration range (0.01–10) ng/mL in 5 mM ($[Fe(CN)_6]^{3-/4-}$).

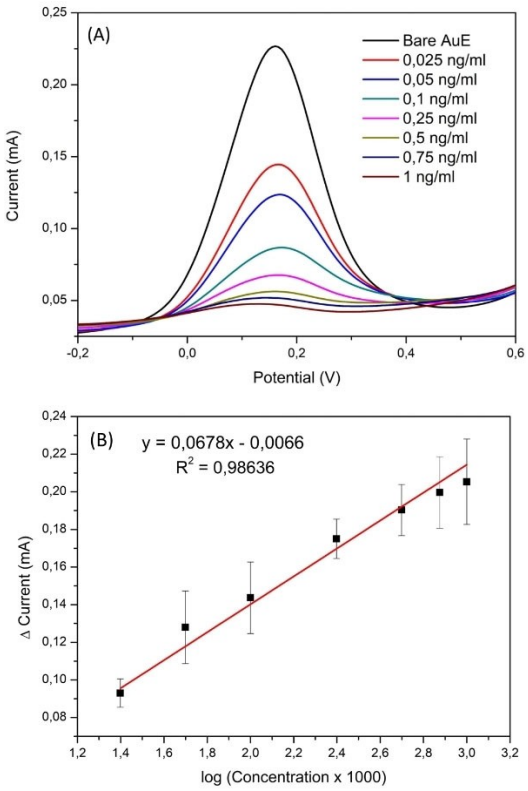


**Figure 3.** (A) Corresponding voltammogram of 7-point calibration curve. (B) 7-point Calibration curve of varied concentration range (0.025–1) ng/mL of SARS-CoV-2 nucleocapsid antibody indicating the linearity of the electrochemical immunosensor in 5 mM ($[Fe(CN)_6]^{3-/4-}$). (n = 3)

An overview of recently reported works for the electrochemical detection of SARS-CoV-2 antibodies is reported in Table 1 highlighting specific biomarkers, bioreceptors, electrode modifiers, and their performance metrics. The analysis includes details on detection sensitivities, analysis times, limits of detection (LOD), and sensing media. Notably, a limited number of studies have focused on SARS-CoV-2 antibody detection, with the majority concentrating on general or spike-protein antibodies. Voltammetric techniques are predominant in current diagnostic procedures, featuring analysis times in the 5–60 min incubation range with only two reported works investigating impedimetric or amperometric approaches. Metal and metal oxide nanoparticle functionalization has commonly been employed to enhance device sensitivity, and alternative substrates such as interdigitated and paper-based platforms have been proposed, showing commendable detection capabilities. Reported detection sensitivities range from fg/mL to μg/mL.

Comparing the designed immunosensor to those reported in Table 1, its simplisity in design and fabrication stands out. The biosensor features a streamlined architecture incorporating a bioreceptor for target recognition and a transducer for signal conversion without the need for further modification with smart materials. The fabrication process involves straightforward steps, making it user-friendly and requiring less specialized skill sets to operate. In contrast to the common RT-PCR, the biosensor can serve as a POC test kit with rapid results availability.

The sensing range for antibody detection spans 0.025 to 1 ng/mL, achieving a low limit of detection (LOD) of 0.019 ng/mL. This level of detection makes the immunosensor suitable for applications demanding high sensitivity, such as medical diagnostics and environmental monitoring. Comparatively, the obtained LOD falls within a reasonable range, competing favourably with the biosensors mentioned and surpassing commercial ELISA test kits. The achieved LOD, however, does not improve detection sensitivity over the only reported electrochemical immunosensor for SARS-CoV-2 nucleocapsid antibodies performed by Sadique et al which may be attributed to the lack of further modification with a graphene-gold nanoparticle nanocomposite. An $R^2$ value of 0.9869 indicates good accuracy in the immunosensor's performance.

**Table 1.** Summary of recent SARS-CoV 2 Antibody Electrochemical sensors reported in literature, highlighting the sensing platform, detection time and LOD.

| Biomarker | Bioreceptor | Sensing Platform | Characterization | Detection time | Limit of detection | Ref |
|---|---|---|---|---|---|---|
| SARS-COV 2 Antibodies | SARS-CoV 2 Antigen | Interdigitated Au NW Impedance gold nanobiosensor | EIS | 20 min | 0,14 pg/ml | [20] |
| SARS-CoV-2 Spike Antibody | SARS-CoV 2 spike Antigen | Glass wafer gold chips | CV | N/A | N/A | [21] |
| SARS-CoV 2 Spike Antibody | SARS-CoV 2 spike Antigen | Graphene oxide paper-based | CV and EIS | 45 min | 1 ng/ml | [22] |
| SARS-CoV 2 Spike Antibody | SARS-CoV 2 spike Antigen | Commercial interdigitated polyethylene terephthalate fused electrodes | EIS | > 5 min | 1 ug/ml | [23] |
| SARS-CoV 2 Spike Antibody | SARS-CoV 2 spike Antigen | Wax paper carbon-based electrode | CA and CV | 13 min | 1,64 ng/ml | [24] |
| SARS-CoV 2 Spike Antibody | SARS-CoV 2 spike Antigen | Nickel hydroxide nanoparticle modified SPCE | CV, EIS and DPV | 20 min | 0,3 fg/ml | [40] |
| SARS-CoV 2 Spike Antibody | SARS-CoV 2 spike Antigen | Gold electrode SAMmix | CV and EIS | 20 min | 1,99 nM | [26] |
| SARS-CoV 2 Spike Antibody | SARS-CoV 2 spike Antigen | Gold nanoparticle-modified SPCE | CV and DPV | 60 min | 75 ng/ml | [27] |
| SARS-CoV 2 Spike Antibody | SARS-CoV-2 spike Antigen | Pentaamine-modified graphene nanoflakes EC Sensor | CV | > 10 min | N/A | [28] |
| SARS-CoV 2 nucleocapsid Antibody | SARS-CoV 2 nucleocapsid protein | Gold nanoparticle Functionalized Graphene Oxide Nanocomposite GCE | CV, EIS and DPV | 5 min | 9,3 ag/ml | [29] |
| SARS-COV 2 Antibodies | SARS-CoV 2 Antigen | Titanium Dioxide Nanoparticle-Based | CV, EIS and DPV | N/A | 3,42 ag/ml | [30] |
| SARS-COV 2 Antibodies | SARS-CoV 2 Antigen | Carbon Nanostructured SPCE | CV | N/A | 2,028ng/mL | [41] |
| SARS-CoV-2 Spike Antibody | SARS-CoV-2 spike Antigen | Gold cluster based GCE | CV,DPV | N/A | 1 fg/ml | [31] |
| SARS-CoV 2 nucleocapsid Antibody | SARS-CoV 2 nucleocapsid protein | Gold electrode | CV,DPV and EIS | 30 min | 0,019ng/mL | This study |

The analysis of test solutions of SARS-CoV-2 N-protein antibodies was performed to validate the viability of the developed method for precise monitoring of antibody concentration. The immunosensor demonstrated an impressive recovery percentage of 96%, signifying high accuracy in detecting and quantifying the target analyte. This result suggests that the immunosensor effectively captures and measures the presence of the desired substance, with minimal loss during the detection process. A high recovery percentage of this magnitude underscores the reliability of the immunosensor and its potential for various applications in fields such as biomedical research and diagnostics.

Furthermore, a response time of 30 min was achieved. Relative to other immunosensors in Table 1, the designed method proves to be efficient. The response time of biosensors is of paramount importance as it directly impacts their real-time detection capabilities. A fast response time ensures rapid and accurate measurement of target analytes. To date, all but one study has conducted detection of SARS-Cov-2 spike protein antibodies utilizing a range of complex platforms. The current work demonstrates that adequate sensitivity for N-protein antibodies using short detection times is possible with no further functionalization.

The reproducibility of the biosensor, as illustrated in Figure 4, is paramount for its practical application and scientific validity. The reproducibility, in this context, refers to the ability of the biosensor to consistently provide accurate and reliable results across multiple tests and experimental setups. The immunosensor displayed relatively reproducible measurements, providing confidence in the ability to replicate findings and compare results effectively. A relative standard deviation percentage of 3.27% was found and signifies the precision of the measured response. The reproducibility observed in the biosensor's performance not only enhances the reliability of the data but also contributes to the credibility of the research outcomes. The ability to consistently generate reliable results reinforces the scientific validity of the immunosensor, making it a robust tool for various applications in research and diagnostics.

The selectivity of the SARS-CoV-2 Nucleocapsid protein as bioreceptor towards its antibody was studied in the presence of SARS-CoV-2-specific IgG and IgM S-protein antibodies. 1 ng/mL of each antibody was incubated at the SARS-CoV-2 Nucleocap-

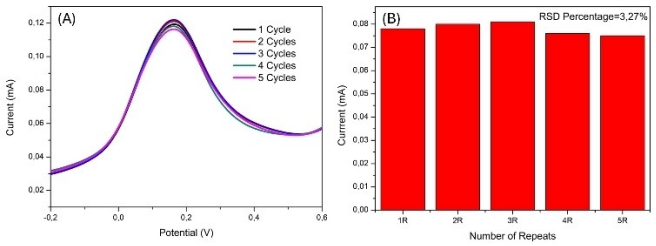


**Figure 4.** (A) Voltametric reproducibility analysis of electrochemical immunosensors of 1 ng/mL SARS-CoV-2 nucleocapsid antibody in 5 mM ($[Fe(CN)_6]^{3-/4-}$), and (B) Bar graph of change in voltammograms consistency and reliability of measurements indicating a relative standard deviation percentage of 3.27%

sid protein functionalized immunosensor and changes in Ferri/ferrocyanide redox probe peak currents measured. The recorded voltammograms are shown in Figure 5. A 33% decrease in peak current is observed in the presence of both S-protein antibodies studied. This change is significantly less than the 90% seen for Nucleocapsid antibody showing its improved binding affinity and selectivity. The partial interference of the spike antibody of SARS-CoV-2 with the nucleocapsid protein is due to the fact that both have IgG responses. Both the Nucleocapsid and Spike Antibody have structural similarities along their peptide sequence that interacts with the nucleocapsid protein.[42,43]

### Synthetic Human Serum Testing

Finally, to demonstrate the practical applicability of the SARS-CoV-2 nucleocapsid Antibody immunosensor, a human serum electrolyte was used for the detection of antibodies. The choice of human serum is practically relevant as common SARS-CoV-2 tests involve sampling blood, saliva, and mucus. Three concentrations of antibodies (0.1, 0.5, and 1 ng/mL) were utilized in the experiment. As depicted in Figure 6, the immunosensor exhibited robust performance, yielding an $R^2$ value of 0.99932. These results collectively suggest that the method offers good precision, trueness, andhigh accuracy. The successful detection of antibodies in a medium as complex as human serum reinforces the practical utility and reliability of the immunosensor in real-world scenarios. This finding further supports the immunosensor's potential as a valuable tool in clinical settings, contributing to the accurate and sensitive detection of SARS-CoV-2 antibodies in patient samples.

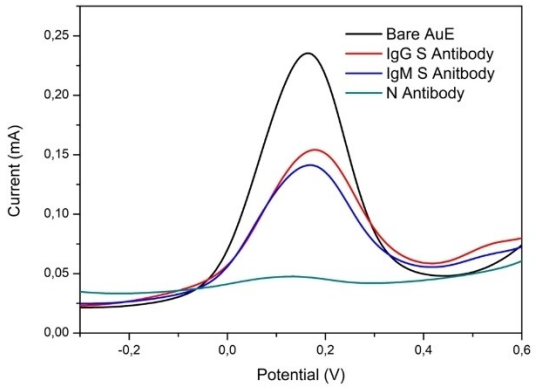


**Figure 5.** Voltametric interference study of 1ng/mL of the IgG and IgM SARS-CoV-2 S proteins compared to 1 ng/mL SARS CoV-2 nucleocapsid antibody in 5 mM ($[Fe(CN)_6]^{3-/4-}$).

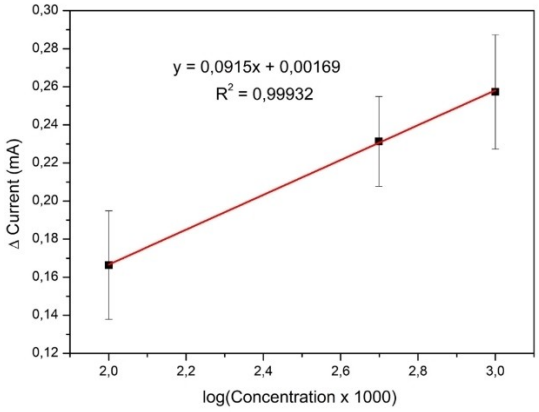


**Figure 6.** Calibration curve of varied concentration range (0.1–1) ng/mL of synthetic human serum detection of SARS- CoV 2 nucleocapsid antibody done in 5 mM ($[Fe(CN)_6]^{3-/4}$). (n = 3)

## Conclusions

To conclude, the development of a SARS-CoV-2 immunosensor holds immense relevance in the context of the ongoing COVID-19 pandemic and beyond. The COVID-19 pandemic has brought significant disruptions to societies worldwide, emphasizing the need for rapid and accurate diagnostic tools to control the spread of the virus. Immunosensors, such as the one developed, have the potential to revolutionize the way we detect and monitor SARS-CoV-2 infections. Herein a label-free electrochemical immunosensor with a simplistic design was capable of detecting SARS-CoV-2 nucleocapsid antibody. The work exhibited only the second study for anti-SARS-CoV-2 N-protein antibodies. The sensing scheme relies on the disruption of the redox conversion ($[Fe(CN)6]^{3-/4-}$) triggered by immunocomplex formation between the captured immunoglobulins produced in response to SARS-CoV-2 in humans with the immobilized nucleocapsid protein of SARS-CoV-2. The fast 30 min and sensitive detection of SARS-CoV-2 antibodies was recorded with a detection limit of 0.019 ng/mL, which is more sensitive than half of the reported antigen-antibody SARS-CoV-2 Immunosensors in the absence of further smart material (nanomaterial, polymer, etc.) modification or use of other complex substrates. In addition, the basic device was capable of detecting targeted antibodies in synthetic human serum and has an acceptable sensitivity and specificity.

The primary advantage of an immunosensor lies in its ability to detect the presence of specific antibodies with high sensitivity and specificity. By harnessing the unique binding properties of antibodies, immunosensors can accurately identify the presence of SARS-CoV-2 in patient samples, even at low concentrations. This feature enables early detection of the virus, which is crucial for timely isolation and treatment, thus limiting the spread of COVID-19. The simplicity of immunosensor technology makes it suitable for point-of-care testing. This means that healthcare professionals can rapidly screen individuals for SARS-CoV-2 infection in various settings. This capability facilitates efficient contact tracing and enables the implementation of targeted measures to control outbreaks. The development of SARS-CoV-2 immunosensors represents a significant breakthrough in the fight against COVID-19 and highlights the potential for transformative diagnostic technologies. With their high sensitivity, specificity, portability, and versatility, immunosensors have the capacity to revolutionize infectious disease detection, surveillance, and prevention not only during the

current pandemic but also in future outbreaks. It is crucial to continue supporting research and innovation in this field to maximize the potential of immunosensors in improving global health and well-being.

## Materials and Methods

### Chemicals and Materials

Palm-sens 4, PalmSens, Houten, The Netherlands. 3 mm Gold Voltammetry (Au) working electrode (MF-2114), Platinum wire Auxiliary electrode (MW-1032), Ag/AgCl with KCl solution reference electrode. Potassium Chloride (SIGMA-ALDRICH), Potassium Ferricyanide (SAARCHEM), MSA (SIGMA-ALDRICH), PBS (CAPRICORN SCIENTIFIC), (1-ethyl-3-(3-dimethylaminopropyl) carbodiimide)(EDC)(SIGMA-ALDRICH), N - Hydroxysuccinimide (NHS) (SIGMA-ALDRICH), N Protein (Sino Biological), BSA (SIGMA-ALDRICH), Antibody (Sino Biological).

### Anti-Sars-Cov-2 Immunosensor Fabrication

All time and concertation optimizations of incubation are available in the supporting information (**SI**). Self-assembled monolayers (SAMs) of mercaptosuccinic acid (MSA) were formed on the Gold (Au) working electrode. To achieve this, a 25 mM MSA solution, prepared in phosphate-buffered saline (PBS), was applied to the working electrode and allowed to incubate for 24 hours. Following the incubation period, the excess MSA solution was carefully removed, and the electrode was rinsed with PBS to eliminate any remaining MSA. For the subsequent cross-linking interaction, a 25 mM solution of EDC-NHS was employed. As indicated by literature, the most effective incubation time for this cross-linking agent was determined to be 30 min, as EDC-NHS tends to be unstable in water for longer periods.[44] A solution containing 10ug/mL of N-Protein, prepared in PBS, was then applied to the electrode and incubated for 1 hour, a parameter optimized through experimentation. To block non-specific binding sites, a 1% bovine serum albumin (BSA) solution was utilized. This BSA solution, composed of 10 mg of BSA in 1 mL biological phosphate buffer, was applied to the device, aligning with literature suggesting that an incubation time of 30 min is sufficient to block most non-specific sites. This step enhances the specificity and selectivity of the biosensor by preventing unwanted interactions.

### Antibody Interacting with Protein

The developed electrochemical immunosensor was applied to the detection of SARS-CoV-2-specific Nucleocapsid antibodies in test solutions. To electrochemically assess the nucleocapsid antibody binding, the electrochemical signal of the functionalized sensor was measured at two key points: first, after the blocking step to establish the background signal, and second, after incubation with the analyte using differential pulse voltammetry (DPV) to obtain the analyte signal. The DPV scans were recorded within the voltage range of −0.5 to 0.7 V. To isolate the specific current change resulting from the antibody binding to the sensor surface, the background signal was subtracted from the analyte signal. This analytical process enhances the precision of the measurements by eliminating non-specific contributions and focusing on the electrochemical response associated with the binding of the nucleocapsid antibody to the sensor surface. The voltammetric analysis was executed using the PS Trace V5.9 software from Palm Sens in Houten, The Netherlands. A schematic illustration of the simple, SARS-CoV-2 immunosensor is shown in Figure 7.

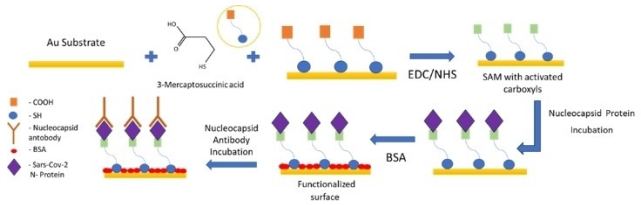


**Figure 7.** Schematic of the preparation of Surface functionalization of the Au electrode for the detection of SARS-CoV-2 nucleocapsid Antibody incubated with the nucleocapsid protein.

### Characterization of Aue Electrochemical Sensor

All the electrochemical measurements were conducted using a portable potentiostat (Palm-sens 4, PalmSens, Houten, The Netherlands). Characterization of the Au electrode was carried out by, differential pulse voltammetry (DPV) and electrochemical impedance spectroscopy (EIS). DPV and EIS were used to characterize the electrode at each stage of the functionalization and to evaluate the antigen-antibody interaction on the surface. All electrochemical measurements were performed in 0.1 M potassium chloride (KCl) solution, containing 5 mM Ferri/ferrocyanide and measured against the Ag/AgCl reference electrode.

## Supporting Information

Assay optimization is included in the supporting information.

## Ethical Compliance

The work was conducted following the University of the Western Cape's Ethical clearance guidelines.

## *Author Contributions*

BJK was responsible for the conceptualization, data acquisition, formal analysis, investigation, validation, and drafting of the

manuscript. He also participated in the review, corrections, and editing. JDP and RAC assisted in data acquisition, formal analysis, and validation. KP and TNPT conceived the study and assisted in the formal analysis, review, and editing of the article, as well as the necessary funding acquisition. NJ and CA assisted in the final review, editing, and clarification of the main ideas in the manuscript.

## Acknowledgements

This study was supported by the South African Medical Research Council (SAMRC) through its Self-Initiated Research (SIR) initiative and the National Research Foundation (NRF) of South Africa (121855).

## Conflict of Interests

The authors declare no conflict of interest.

**Keywords:** Electrochemical Immunosensor · Label-free · SARS-CoV-2 · Nucleocapsid Antibody · Nucleocapsid Protein

[1] T. P. Velavan, C. G. Meyer, *Trop. Med. Int. Health* **2020**, *25*, 278.
[2] Y. H. Jin, L. Cai, Z. S. Cheng, H. Cheng, T. Deng, Y. P. Fan, C. Fang, D. Huang, L. Q. Huang, Q. Huang, Y. Han, B. Hu, F. Hu, B. H. Li, Y. R. Li, K. Liang, L. K. Lin, L. S. Luo, J. Ma, L. L. Ma, Z. Y. Peng, Y. B. Pan, Z. Y. Pan, X. Q. Ren, H. M. Sun, Y. Wang, Y. Y. Wang, H. Weng, C. J. Wei, D. F. Wu, J. Xia, Y. Xiong, H. B. Xu, X. M. Yao, Y. F. Yuan, T. S. Ye, X. C. Zhang, Y. W. Zhang, Y. G. Zhang, H. M. Zhang, Y. Zhao, M. J. Zhao, H. Zi, X. T. Zeng, Y. Y. Wang, X. H. Wang, *Mil. Med.* **2020**, *7*, 1–23.
[3] T. Ai, Z. Yang, H. Hou, C. Zhan, C. Chen, W. Lv, Q. Tao, Z. Sun, L. Xia, *Radiology* **2020**, *296*, E32–E40.
[4] A. Singh, A. Sharma, A. Ahmed, A. K. Sundramoorthy, H. Furukawa, S. Arya, A. Khosla, *Biosensors* **2021**, *11*, DOI 10.3390/bios11090336.
[5] S. Eissa, H. A. Alhadrami, M. Al-Mozaini, A. M. Hassan, M. Zourob, *Microchim. Acta* **2021**, *188*, 1–10.
[6] F. Curti, S. Fortunati, W. Knoll, M. Giannetto, R. Corradini, A. Bertucci, M. Careri, *ACS Appl. Mater. Interfaces* **2022**, *14*, 19204–19211.
[7] L. R. G. Silva, J. S. Stefano, L. O. Orzari, L. C. Brazaca, E. Carrilho, L. H. Marcolino-Junior, M. F. Bergamini, R. A. A. Munoz, B. C. Janegitz, *Biosensors* **2022**, *12*, 622.
[8] B. Mojsoska, S. Larsen, D. A. Olsen, J. S. Madsen, I. Brandslund, F. Alzahra'a Alatraktchi, *Sensors* **2021**, *21*, 390 DOI 10.3390/s21020390.
[9] M. Alafeef, K. Dighe, P. Moitra, D. Pan, *ACS Nano* **2020**, *14*, 17028–17045.
[10] A. Yakoh, U. Pimpitak, S. Rengpipat, N. Hirankarn, O. Chailapakul, S. Chaiyo, *Biosens. Bioelectron.* **2021**, *176*, DOI 10.1016/J.BIOS.2020.112912.
[11] Y. Peng, Y. Pan, Z. Sun, J. Li, Y. Yi, J. Yang, G. Li, *Biosens. Bioelectron.* **2021**, *186*, DOI 10.1016/J.BIOS.2021.113309.
[12] V. J. Vezza, A. Butterworth, P. Lasserre, E. O. Blair, A. MacDonald, S. Hannah, C. Rinaldi, P. A. Hoskisson, A. C. Ward, A. Longmuir, S. Setford, E. C. W. Farmer, M. E. Murphy, D. K. Corrigan, *Chem. Commun.* **2021**, *57*, 3704–3707.
[13] C. Cristea, A. Florea, M. Tertis, R. Sandulescu, in *Biosensors – Micro and Nanoscale Applications*, InTech, **2015**.
[14] J. du Plooy, N. Jahed, E. Iwuoha, K. Pokpas, *R. Soc. Open Sci.* **2023**, *10*, 230940.
[15] F. Mollarasouli, S. Kurbanoglu, S. A. Ozkan, *Biosensors* **2019**, *9*, DOI 10.3390/bios9030086.
[16] M. Y. Wang, R. Zhao, L. J. Gao, X. F. Gao, D. P. Wang, J. M. Cao, *Front. Cell. Infect. Microbiol.* **2020**, *10*, DOI 10.3389/fcimb.2020.587269.
[17] Y. He, Y. Zhou, H. Wu, Z. Kou, S. Liu, S. Jiang, *J. Clin. Microbiol.* **2004**, *42*, 5309–5314.
[18] P. S. Masters, L. S. Stunnan, **n.d**.
[19] Y.-H. Li, J. Li, X.-E. Liu, L. Wang, T. Li, Y.-H. Zhou, H. Zhuang, *J. Virol. Methods* **2005**, *130*, 45–50.
[20] D. I. Sandoval Bojórquez, Ž. Janićijević, B. Palestina Romero, E. S. Oliveros Mata, M. Laube, A. Feldmann, A. Kegler, L. Drewitz, C. Fowley, J. Pietzsch, J. Fassbender, T. Tonn, M. Bachmann, L. Baraban, *ACS Sens.* **2023**, *8*, 576–586.
[21] D. Najjar, J. Rainbow, S. Sharma Timilsina, P. Jolly, H. de Puig, M. Yafia, N. Durr, H. Sallum, G. Alter, J. Z. Li, X. G. Yu, D. R. Walt, J. A. Paradiso, P. Estrela, J. J. Collins, D. E. Ingber, *Nat. Biomed. Eng.* **2022**, *6*, 968–978.
[22] A. Yakoh, U. Pimpitak, S. Rengpipat, N. Hirankarn, O. Chailapakul, S. Chaiyo, *Biosens. Bioelectron.* **2021**, *176*, DOI 10.1016/j.bios.2020.112912.
[23] M. Z. Rashed, J. A. Kopechek, M. C. Priddy, K. T. Hamorsky, K. E. Palmer, N. Mittal, J. Valdez, J. Flynn, S. J. Williams, *Biosens. Bioelectron.* **2021**, *171*, DOI 10.1016/j.bios.2020.112709.
[24] R. Peng, Y. Pan, Z. Li, Z. Qin, J. M. Rini, X. Liu, *Biosens. Bioelectron.* **2022**, *197*, DOI 10.1016/j.bios.2021.113762.
[25] Z. Rahmati, M. Roushani, H. Hosseini, H. Choobin, *Microchem. J.* **2021**, *170*, 106718.
[26] V. Liustrovaite, M. Drobysh, A. Rucinskiene, A. Baradoke, A. Ramanaviciene, L. Plikusiene, U. Samukaite-Bubniene, R. Viter, C. Chen, A. Ramanavicius, *J. Electrochem. Soc.* **2022**, *169*, 037523. DOI 10.1149/1945-7111/ac5d91.
[27] B. A. Braz, M. Hospinal-Santiani, G. Martins, J. L. Gogola, M. G. P. Valenga, B. C. B. Beirão, M. F. Bergamini, L. H. Marcolino-Junior, V. Thomaz-Soccol, C. R. Soccol, *Talanta* **2023**, *257*, 124348.
[28] S. S. Timilsina, N. Durr, P. Jolly, D. E. Ingber, *Biosens. Bioelectron.* **2023**, *223*, 115037.
[29] M. A. Sadique, S. Yadav, P. Ranjan, R. Khan, F. Khan, A. Kumar, D. Biswas, *ACS Appl. Bio Mater* **2022**, DOI 10.1021/acsabm.2c00301.
[30] M. A. Sadique, S. Yadav, V. Khare, R. Khan, G. K. Tripathi, P. S. Khare, *Diagnostics* **2022**, *12*, 2612.
[31] L. Liv, H. Kayabay, *ChemistrySelect* **2022**, *7*, e202200256.
[32] N. Kumar, N. P. Shetti, S. Jagannath, T. M. Aminabhavi, *Chem. Eng. J.* **2022**, *430*, 1385–8947.
[33] M. Döhla, C. Boesecke, B. Schulte, C. Diegmann, E. Sib, E. Richter, M. Eschbach-Bludau, S. Aldabbagh, B. Marx, A.-M. Eis-Hübinger, R. M. Schmithausen, H. Streeck, *Public Health* **2020**, *182*, 170-172. DOI 10.1016/j.puhe.2020.04.009.
[34] Q. Wu, W. Wu, F. Chen, P. Ren, *Analyst* **2022**, *147*, 2809-2818. DOI https://doi-org.ezproxy.uwc.ac.za/10.1039/D2AN00426G.
[35] B. S. Vadlamani, T. Uppal, S. C. Verma, M. Misra, *Sensors* **2020**, *20*, 1–10.
[36] Y. Peng, Y. Pan, Z. Sun, J. Li, Y. Yi, J. Yang, G. Li, *Biosens. Bioelectron.* **2021**, *186*, DOI 10.1016/j.bios.2021.113309.
[37] D. Soto, J. Orozco, *Anal. Chim. Acta* **2022**, *1205*, 339739. DOI 10.1016/j.aca.2022.339739.
[38] M. D. T. Torres, W. R. de Araujo, L. F. de Lima, A. L. Ferreira, C. de la Fuente-Nunez, *Matter* **2021**, *4*, 2403–2416.
[39] G. Seo, G. Lee, M. J. Kim, S. H. Baek, M. Choi, K. B. Ku, C. S. Lee, S. Jun, D. Park, H. G. Kim, S. J. Kim, J. O. Lee, B. T. Kim, E. C. Park, S. Il Kim, *ACS Nano* **2020**, *14*, 5135–5142.
[40] Z. Rahmati, M. Roushani, H. Hosseini, H. Choobin, *Microchem. J.* **2021**, *170*, 106718.
[41] J. du Plooy, B. Kock, N. Jahed, E. Iwuoha, K. Pokpas, *Molecules* **2023**, *28*, 8022.
[42] H. R. Choudhary, D. Parai, G. C. Dash, A. Peter, S. K. Sahoo, M. Pattnaik, U. K. Rout, R. R. Nanda, S. Pati, D. Bhattacharya, *Infection* **2021**, *49*, 1045–1048.
[43] "The interaction of the antibody molecule with specific antigen, https://www.ncbi.nlm.nih.gov/books/NBK27160/#:~:text=The%20surface%20of%20the%20antibody,surfaces%20created%20by%20these%20CDRs," **n.d**.
[44] X. Zhang, X. Liao, Y. Wu, W. Xiong, J. Du, Z. Tu, W. Yang, D. Wang, *Anal. Bioanal. Chem.* **2022**, *414*, 1129–1139.

Manuscript received: March 27, 2024